NTNU – Trondheim
Norwegian University of
Science and Technology

Monte Carlo simulations of neutron fluence through concrete wall in proton therapy

John Alfred Brennsæter

December 2014

PROJECT THESIS

Department of physics

Norwegian University of Science and Technology

Supervisor: Associate Professor Pål Erik Goa

Preface

This Projects assignment in medical physics at NTNU is part of the study program Biophysics and medical technology. This project has been carried out during the autumn semester of 2014. The idea to the project was brought up by Associate Professor Pål Erik Goa in cooperation with Project Manager Odd Harald Odland at Haukeland University Hospital and Professor Dieter Röhrich at the University in Bergen.

Trondheim, 2014-12-19

John Alfred Brennsæter

Acknowledgment

I would like to thank the following persons for their help during the project.

Project Manager Particle Therapy Odd Harald Odland at Department of Oncology and Medical Physics Haukeland University Hospital for professional input in the starting phase of the project.

Professor Dieter Röhrich at the Department of Physics University in Bergen for professional input and adjustments when defining the project.

Kristian Smeland Ytre-Hauge for great help with FLUKA-simulations.

Sigrun Saur Almberg, Jomar Frengen and the Clinic of Oncology St. Olavs Hospital for their supportive interest.

Eivind Rørvik for professional conversations and discussions and cooperation during the project.

Finally, I would like to to thank my supervisor Associate Professor Pål Erik Goa for great support during the entire project.

J.A.B.

Sammendrag

Protonterapi er en sterkt voksende gren av stråleterapi. I 2012 ble det bestemt at det norske pasienter skal få tilbud om protonterapi. Protonterapi benytter seg av protoner som blir akselerert opp til energier mellom 70 MeV og 250 MeV. Dette fører til en stor økning i dannelse av sekundære partikler sammenlignet med fotoner, og det fører til økt energi til de partiklene som blir dannet. Nøytroner krever spesiell oppmerksomhet siden de er uladd og dermed kan bevege seg vesentlig lenger enn ladde partikler før de stopper. Dette fører til at det kreves strengere sikkerhetsreguleringer når det kommer til strålevern for protonterapi. Dette arbeidet har undersøkt hvordan nøytronfluencen fra nøytroner dannet av kjernereaksjoner mellom protoner og et vannfantom attenueres gjennom en betongvegg ved hjelp av Monte Carlo simuleringer.

Simuleringene i dette prosjektet har blitt utført med Monte Carlo simuleringsverktøyet FLUKA. Et vannfantom på 100 cm x 30 cm x 40 cm har blitt bestrålt av en protonstråle med varierende energi fra 70 MeV til 250 MeV. Nøytronfluence og energispektre har blitt detektert.

Simuleringene viste at nøytronfluencen er sterkt avhengig av protonstråleenergien. Det blir generert vesentlig flere nøytroner som når fram til veggen og de nøytronene som når fram har vesentlig høyere energi, når protonstråleenergien øker. Det fører til at den relative forskjellen i nøytronfluence mellom de forskjellige protonstråleenergiene øker jo dypere inn i veggen man kommer. Grunnen til dette er at nøytroner med høyere energi trenger flere kollisjoner for å bli redusert til en energi hvor det er sannsynlig å bli fanget opp av et atom og stoppe, i tillegg er det større sannsynlighet for at de genererer nye partikler blandt annet nøytroner ved nye kjernereaksjoner. Energispekteret følger samme mønster opp til 10 MeV, uansett protonstråleenergi, ved overflaten av veggen. Andelen nøytroner med høyere energi øker betraktelig når protonstråleenergien øker. Lenger inn i veggen ble statistikken fort for dårlig til å kunne si noe eksakt om energispekteret. Dette burde vært løst ved hjelp av biasing, en teknikk som forbedrer statistikken i valgte regioner, uten å jukse med fysikken.

Abstract

Proton therapy is a growing branch of radiation therapy. In 2012 it was decided that norwegian patients should be offered proton therapy treatment. Proton therapy utilizes protons accelerated up to energies in the range of 70 Mev to 250 MeV. This leads to a significant increase in generation of secondary particles compared to photon therapy, and the generated particles may have higher energy. Neutrons demands special attention since they are uncharged and therefore might traverse significantly longer through matter before they are captured and surrender their energy. This work has investigated how the neutron fluence originated from nuclear interactions in a water phantom irradiated by a proton beam attenuates through a concrete wall for different proton beam energies by Monte Carlo simulations.

The simulations in this project has been performed with the FLUKA Monte Carlo tool. A water phantom with the dimensions of 100 cm x 30 cm x 40 cm has been irradiated by a proton beam with varying energies from 70 MeV to 250 MeV. Neutron fluence and energi spectra have been detected.

The simulations showed that the neutron fluence is strongly dependent of the proton beam energy. Significantly more neutrons are generated and there are more high energy neutrons, when the proton beam energy increases. This leads to that the relative difference in neutron fluence for different proton beam energies is increasing deeper into the wall. This is due to neutrons with higher energy needs more collisions to be reduced to an energy where radiative capture is probable. In addition, the probability of nuclear interactions where more neutrons are generated increases with higher neutron energy. The energy spectra for the different proton beam energies follows the same pattern up to 10 MeV, at the surface of the wall. The share of high energy neutrons increases significantly when the proton beam energy increases. Farther into the wall the statistics are worsening with reduced fluence. This makes the energy spectrum hard to interpret as the uncertainty is too high. This should have been solved by using biasing, a technique that improves the statistics in chosen region without changing the physics.

Contents

Chapter 1

Introduction

Throughout the last century radiation therapy with photons has grown to be a central part of cancer treatment. However, the last decades there has been an exponential increase in the use of proton beams in radiation therapy. In 2012 the norwegian Ministry of Health and Care Services commisioned the Directorate of Health to establish facilities to serve norwegian patients with proton therapy. It has not yet been decided when and where the facilities will be built, but it is expected that the first patient may be treated around 2020.

Proton therapy centers are expensive compared to conventional photon therapy centers, but the cost is justified by the superior depth dose distribution for protons (Suit H. et al. 2003). This may lead to a lower dose to organs at risk under proton therapy compared to photon therapy.

Proton therapy makes use of much higher energies than conventional photon therapy. Secondary particles, and then specially neutrons give rise to radiation exposure to the environment. When the beam energy increases the amount of secondary particles increases as well. In addition, the energy of the secondary particles also increases. This leads to higher security requirements when it comes to shielding of the treatment rooms. The treatment rooms are usually shielded by thick concrete walls to ensure that the radiation exposure to the environment is below an acceptable level. The objective of this work is to investigate the neutron fluence through a concrete wall from neutrons originated from a proton beam irradiating a water phantom by Monte Carlo simulations for different proton beam energies.

Chapter 2

Theory

2.1 Interactions between protons and matter

When a proton beam is irradiating a material, as human tissue or a water phantom, the particles will interact with the particles in the material. There are mainly three reactions that dominates; stopping, scattering and nuclear interaction (Gottschalk, 2012).

2.1.1 Stopping

Stopping is caused by the protons interacting with atomic electrons. The protons interact with electrons during the entire way through the material, but as the velocity decreases, the time the proton is within the range of a single electron increases. Hence, the energy transfer is increased. This leads to the characteristic Bragg peak for heavy charged particles, a sharp increase in dose at a distance determined by the energy of the proton.

2.1.2 Scattering

Scattering is caused by electrostatic Coloumb interactions between the protons and atomic nuclei. These interactions are elastic nuclear reactions. The scattering angle increases for nuclei with high atomic mass.

2.1.3 Nuclear Interactions

Nuclear interacions is caused by protons colliding with atomic nuclei causing a nonelastic nuclear reaction. Protons enter the nucleus and interact with it, and another nucleon is released. For low energy protons, the electrostatic repulsion between the proton and the nucleon prevents this from happening, but this is negligable for proton energies much larger than 100 keV (Tavernier, 2010). Nuclear reactions are in this report denoted as (i,e), where i is the incoming particle and e is the emitted particle. The emitted particle can be a proton, neutron or a cluster of nucleons and are called secondary particles or secondaries. The biological effect of the generation of secondary particles is small(Gottschalk, 2012). However, the secondary particles move on and will transfer their energy other places. While the scattered protons typically change the direction with only a few degrees, the secondary particles may make a large angle with the beam (Gottschalk, 2012).

2.2 Interactions between neutrons and matter

While protons and other charged particles reacts strongly with matter, neutrons is significantly less reactive. Neutrons have no charge and can therefore travel a much longer distance. Neutrons with different energies interact differently. The different neutron classes are shown in table 2.1.

Neutrons interact with matter when they collide with other atoms. This can be either an inelastic or elastic reaction. For the elastic reactions the kinetic energy is conserved, but for the inelastic reactions the nucleus the neutron collides with is left in an excited state. Hence, the inelastic scattering threshold equals the lowest excited state of the material. A neutron can also be captured in reactions like (n,γ), (n,2n) and several other reactions (Paganetti, 2012).

Table 2.1: Neutron energy classification

Class	Energy range
Thermal	$E_n < 0.5$ eV
Intermediate	0.5 eV $< E_n <$ 10 keV
Fast	10 kev $< E_n <$ 20 MeV
Relativistic	$E_n > 20$ MeV
High-energy	$E_n > 100$ MeV

2.2.1 Relativistic neutrons

Neutrons with energies above 50 MeV regenerates lower energy neutrons by nuclear reactions. Neutrons can interact with a single nucleon in the nucleus and thereby evaporate other particles from the nucleus. When there is no more energy left for particle emission, the rest of the excitation energy is released as a gamma ray. However, the nucleus may still be radioactive.

2.2.2 Fast neutrons

Fast neutrons may also regenerate more neutrons. Their energy are reduced by several elastic and inelastic reactions, until they are reduced to intermediate and then thermal neutrons or undergo radiative capture (n,γ). As the energy decreases the probability for inelastic reactions decreases. Inelastic reactions dominates for energies above 10 MeV, while there are almost only elastic scattering for neutron energies below 1 MeV.

2.2.3 Thermal neutrons

The neutrons with lowest energy are called thermal neutrons. The name is based on the fact that they are in approximate equilibrium with the surrounding particles. Thermal neutrons do only interact with other atoms by elastic scattering, because they do not have enough energy to excite other atoms. They diffuse about, until they undergo radiative capture.

2.3 General Aspects of Proton Therapy

In proton therapy protons are accelerated by either a cyclotron or a synchrotron. A cyclotron is accelerating the protons in a constant magnetic field by a varying electric field. The protons follows a spiral path until they reach the velocity that make them escape from the magnetic field into the beam line. A synchrotron is accelerating protons following a constant path. The protons are accelerated by a linear accelerator and bending magnets turns the beam around and through the linear accelerator several times, until the protons have the desired energy and another magnet leads them in to the beam line. The synchrotron has the advantage that it is possible to choose the wanted energy directly, while the cyclotron can only deliver protons at

one energy. When the protons have been accelerated, they are directed towards the treatment room by other bending magnets.

To distribute the proton beam in the target volume there is at the moment two different techniques. The simplest technique, called passive scattering, uses metal scatterers in the beam line and collimators which provides a evenly distributed beam over the entire target volume. The scatter material should give high scattering, low absorption and generate few secondary particles. In addition to the scatterers there is also a range modulator. This consists of a material that the beam goes through. This is often solved with a rotating wheel with varying thickness. This creates the spread out Bragg-peak which is wanted for getting a homogenous dose for the target voulme. For the range modulator it is desirable to have a material that gives high absorption and low scattering and also generates as few as possible secondary particles.

The more modern technique, called active scanning, utilizes magnets to steer the proton beam accurately towards the tumor and scan the tumor layer by layer. This removes a lot of materials from the beam line compared to passive scattering, which is favorable because it reduces the number of secondary particles.

2.4 Fluence

If N particles passes through an area A, the fluence, Φ, for that area is then

$$\Phi = \frac{N}{A} \tag{2.1}$$

2.5 Monte Carlo Simulations

Monte Carlo simulations is used to predict the outcome of an experiment. The geometry of the experiment are modelled and the result is statistically predicted based on a high number of random histories. The statistics of the prediction is decided from probability distributions which is determined by the different possible physical interactions. Radiation therapy is well suited for Monte Carlo simulations as each particle is an independent history that can be simulated.

Today Monte Carlo simulation is mainly a research tool, and is rarely used in clinics. This is

primarily because it is considered too time consuming if the detail level of the simulations is on an acceptable level. However, this might be changing during the coming years as the computational power are getting higher.

2.5.1 Biasing

Biasing is a technique to vary the number of histories to track based on the importance of the region in Monte Carlo simulations.

Russian roulette

Russian roulette is a technique that changes the factor of histories in a region reducing the probability of the particle crossing the boarder to that region by a factor. However, the physics are unchanged, as the particles that do cross the border is weighted accordingly to the reduction.

Splitting

Splitting is an other type of biasing, that changes the particles that crosses the boarder to a region to several particles. The physics are kept right in this situation as well by changing the weighting of each particle.

Chapter 3

Materials and Methods

The Monte Carlo simulations in this project have been performed with the FLUKA Monte Carlo tool (Battistoni et al., 2007). FLUKA is a Monte Carlo code used in particle physics.

The neutron cross sections in FLUKA are continuosly updated from the most recent evaluations(ENDF, JEFF, JENDL). Low energy neutrons, below 20MeV, are treated with a cross section library of 260 energy groups.

In FLUKA ion interactions are handled seperately based on the energy of the ions.Ions with energy less than 0.1GeV are handled with Boltzmann Master Equation (BME) Theory, while ions with energy between 0.1GeV and 5GeV are handled with Relativistic Quantum Molecular Dynamics Model (RQMD) (F. Cerutti, 2010).

The Monte Carlo simulations were performed using a regular Linux laptop. Five independent simulations with 10^6 or 10^5 primary particles were performed for each Monte Carlo set-up. For energies up to 190MeV 10^6 primary particles, and for the highest energies 10^5 primary particles were simulated. This was due to increasing computing time with higher energies.

A Gauss-shaped beam with FWHM at 1.0 cm in both lateral directions was used as input for the FLUKA Monte Carlo simulations. Neutron fluence estimates and neutron energy spectra have been obtained for varying proton beam energies from 70MeV to 250MeV with intervals of 30MeV.

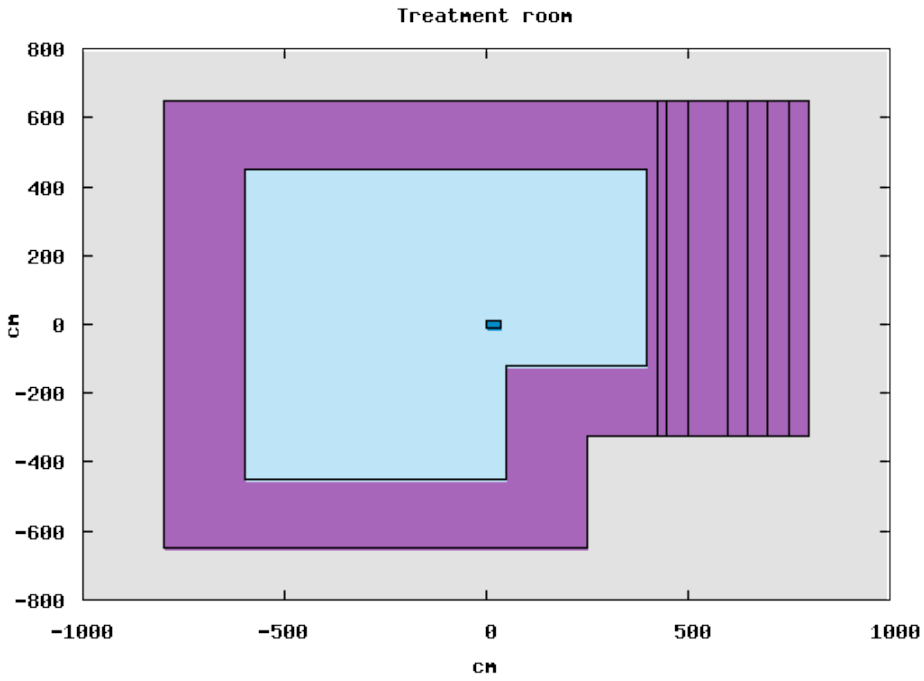

Figure 3.1: zy-projection of the model of the treatment room used in the simulations. This includes a water phantom, air in the treatment room and concrete walls surrounding the treatment room. The wall perpendicular to the beam axis is seperated in different regions, to measure the energy spectrum of the fluence crossing the boundaries between the regions.

Treatment room

The treatment room in the FLUKA simulations are based on technical drawings from a vendor. However, there are no gantry in the geometry. The treatment room are filled with air. The walls consists of a concrete material pre-defined in FLUKA.

Phantom

The proton beam has irradiated a water phantom of (100 cm x 30 cm x 40 cm). The phantom is 40 cm in the depth direction. This ensures that the Bragg peak is inside the phantom for all proton beam energies.

3.1 Scoring

The fluence of the neutrons in the concrete wall has been obtained by using the Usrbin scoring card. This card can be utilized to detect the trace of each neutron in a specific region.

The energy spectrum of the neutrons that passes through different planes in the wall, has been obtained by using the Usrbdx scoring card. This card detects the energy of each particle that passes through the boundary between to regions. The energy spectra is plotted in isolethargic units. This means that the spectra is plotted as

$$\frac{d\Phi}{d(\log E)} = E\frac{d\Phi}{dE} \tag{3.1}$$

This gives a more intuitive view of the results when the spectra are plotted with logarithmic x-axis as the area beneath the graph then is proportional to fluence.

Chapter 4

Results

4.1 Neutron fluence

The neutron fluence through the concrete wall are shown in figure 4.1. The results shows that there is generated significantly more neutrons that reach the treatment wall for higher energy proton beams. Figure 4.2 shows the difference in attenuation for different proton beam energies. It is evident that the neutron fluence is attenuated faster for lower energy proton beams.

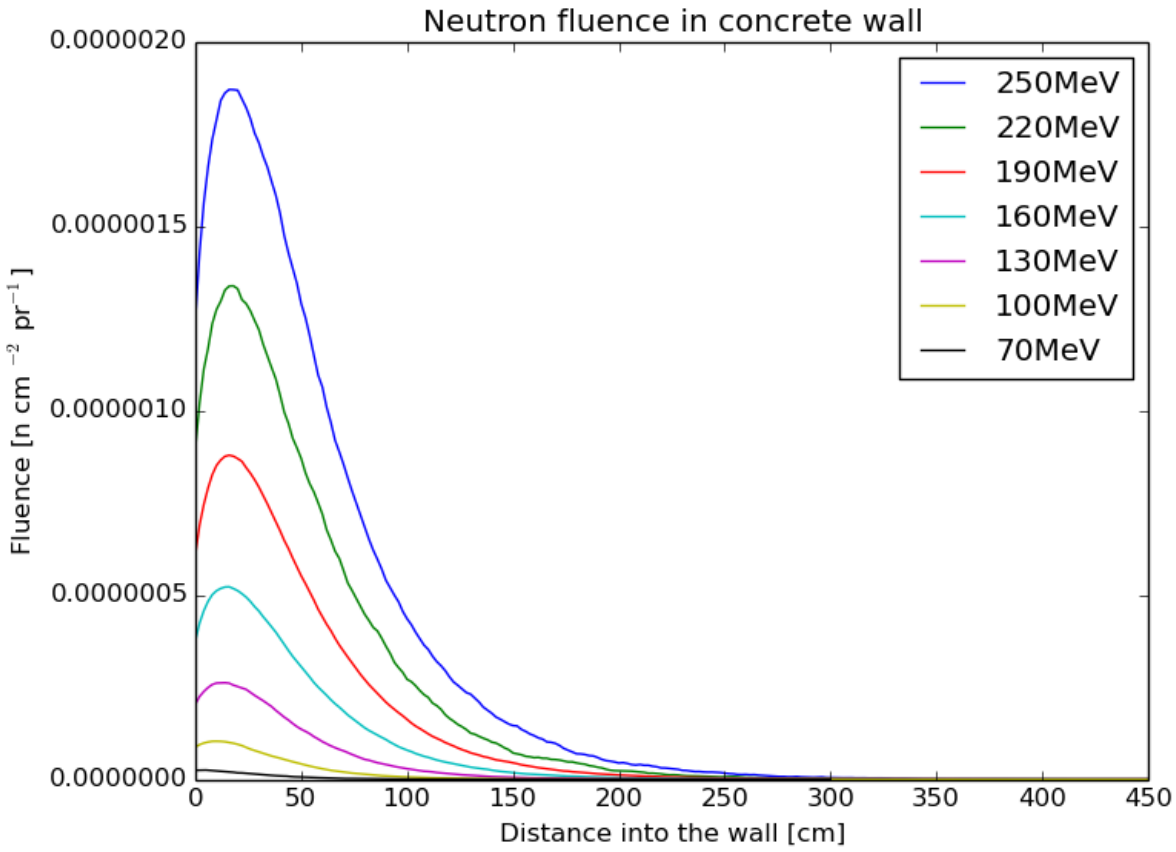

Figure 4.1: Neutron fluence per primary proton as a function of depth into the wall for different proton energies.

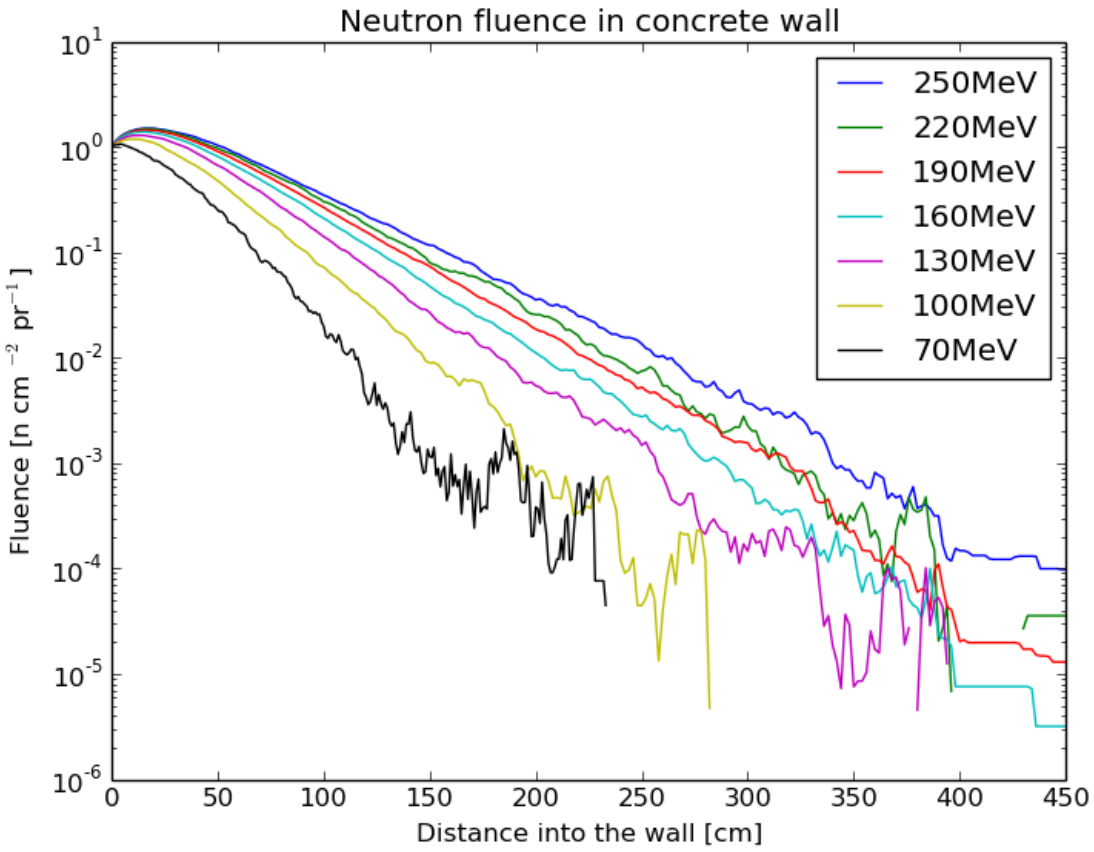

Figure 4.2: The figure shows the neutron fluence developement when the incoming neutron fluence is 1 n cm^{-2}, as a function of depth into the wall for different proton beam energies.

4.2 Energy spectra

The energy spectra of the neutrons at the surface of the wall are shown in figure 4.3. The spectra are normalized to make the comparison easier. We can see that the energy spectra follows the same pattern until the high energy peak, where the shape and the magnitude of the peak differs. Figure 4.4 shows the different shapes of the high energy peaks. The maximum neutron energy is limited by the proton beam energy.

The energy spectra of the neutrons at 100 cm depth is shown in figure 4.5. Although the statistics are not perfect it is evident that the energy spectra for the different proton beam energies still follows the same pattern for lower energies. As we take a closer look at the higher energies in figure 4.6, we can see that the shape of the high energy peak at 100 cm depth has almost the same shape for all energies, only seperated by a maximum energy corresponding to the proton beam energy. The statistics are not good.

The energy spectra of the neutrons at 200 cm depth is shown in figure 4.7. We can see that the statistics for the measurements are bad.

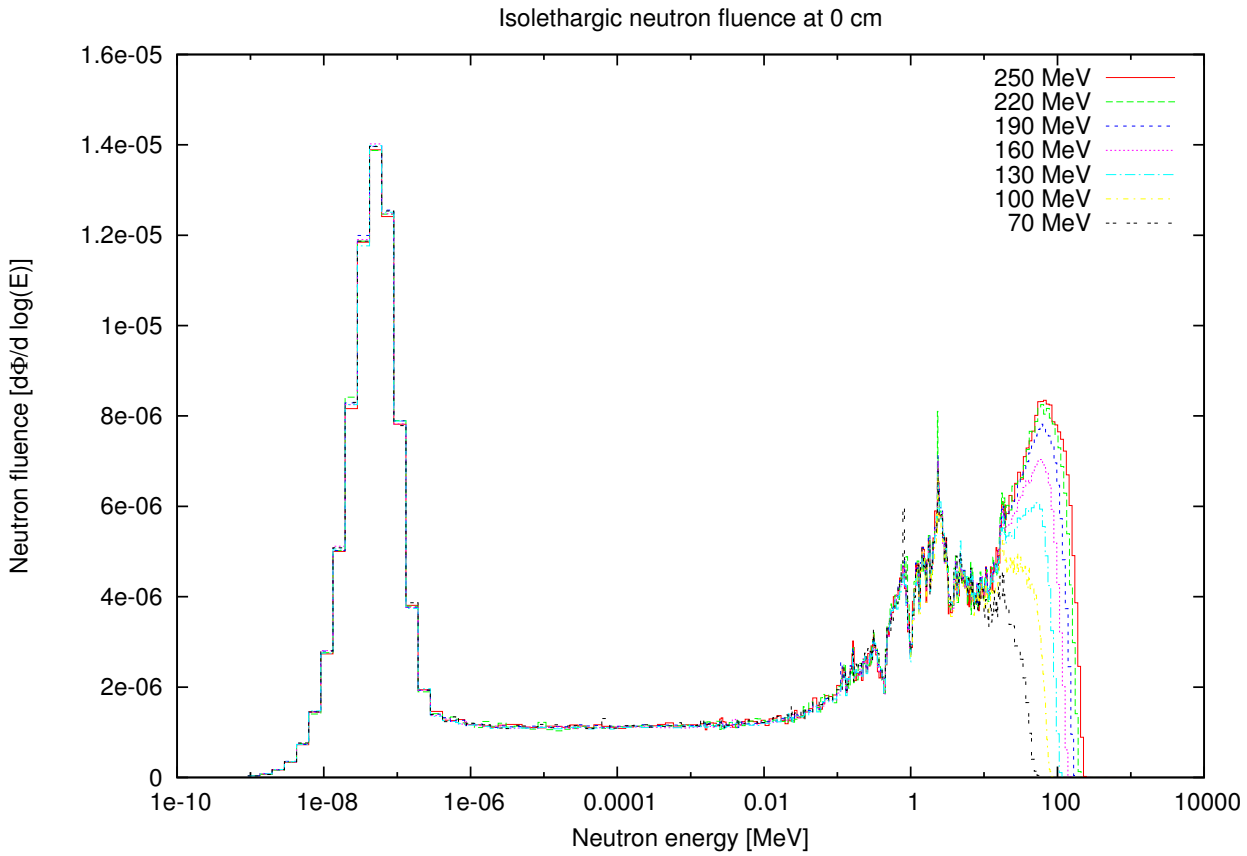

Figure 4.3: Energy spectrum for neutrons at the surface of the wall for different proton beam energies. The spectra are normalized for comparison so the neutron fluence does not correspond to the same number of primary protons.

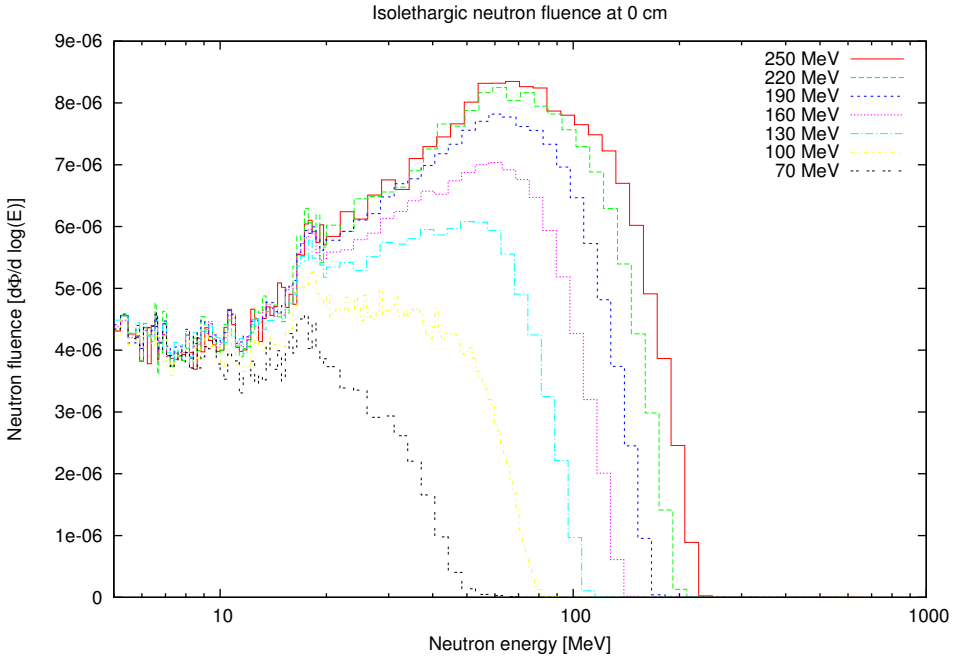

Figure 4.4: Energy spectra for neutrons at the surface of the wall for different proton beam energies for neutron energies above 5 MeV.

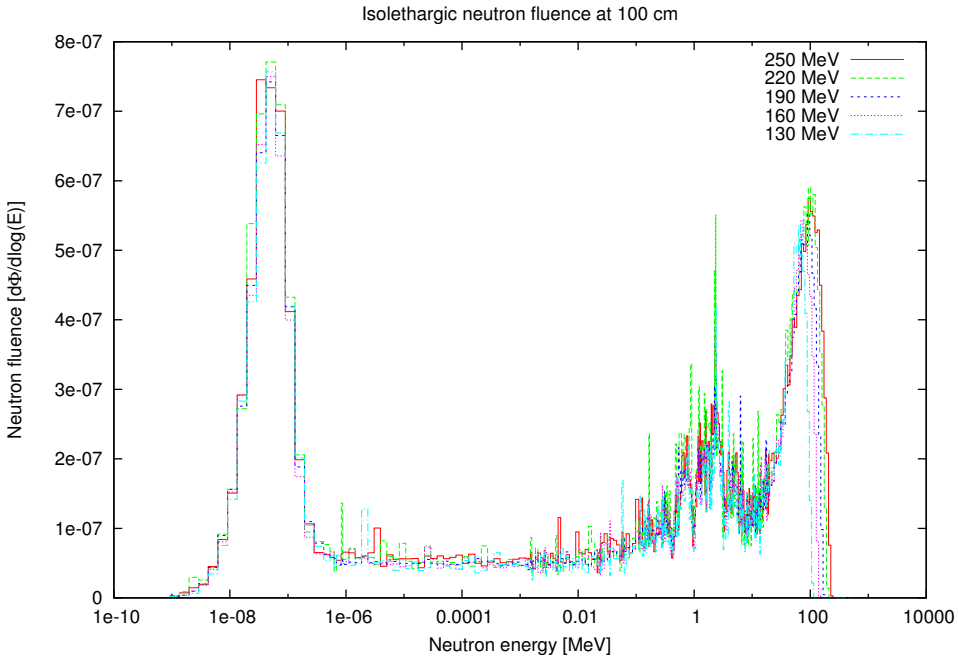

Figure 4.5: Energy spectra 100 cm into the wall.

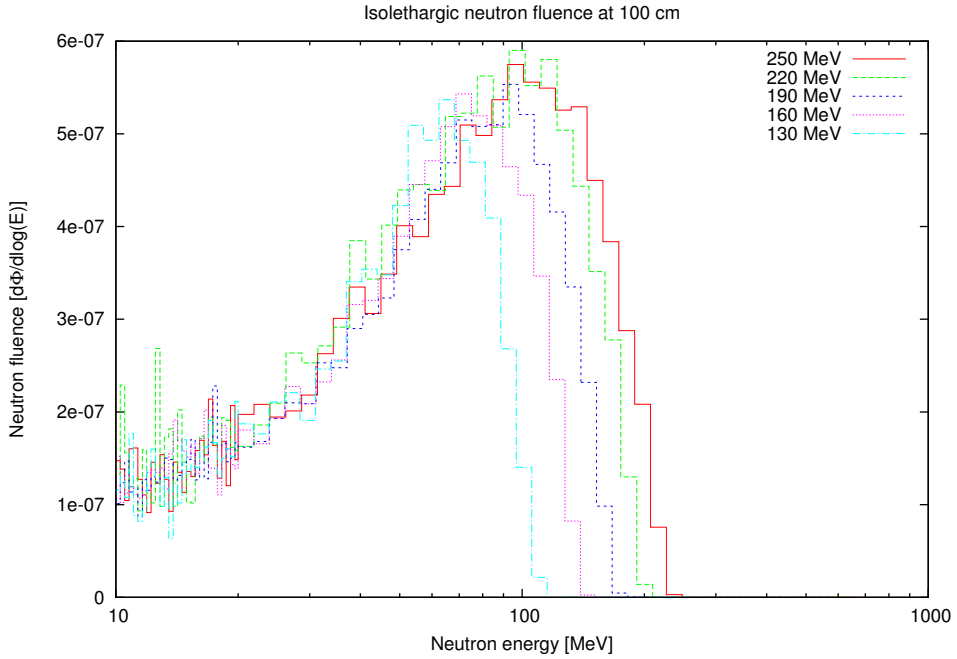

Figure 4.6: Energy spectra 100 cm into the wall for energies above 10 MeV.

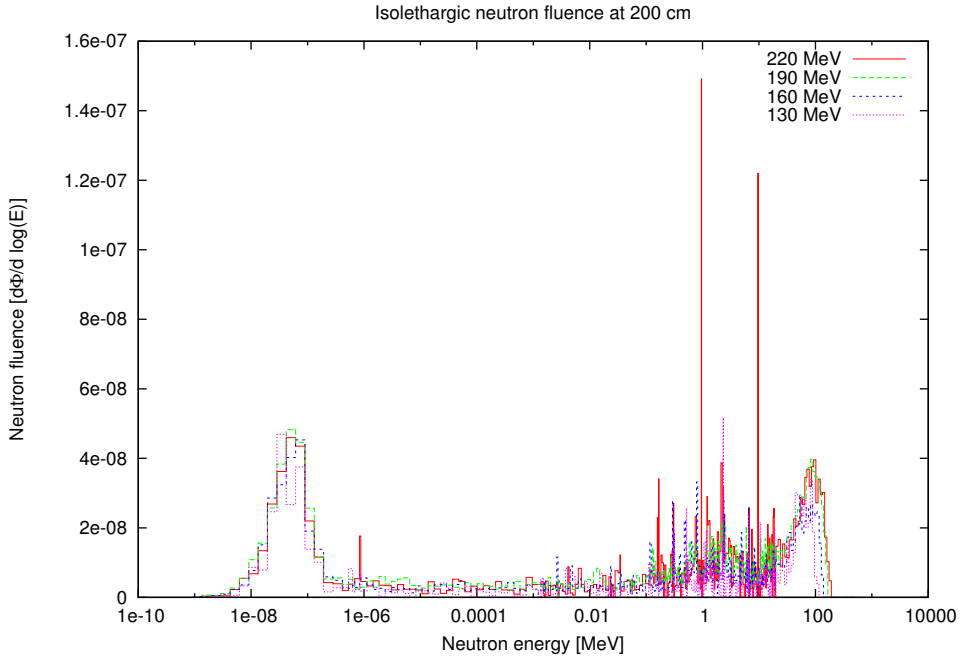

Figure 4.7: Energy spectrum for neutrons 200 cm into the wall for different proton beam energies.

Chapter 5

Discussion

The setup for this experiments gives some limitations for the information in results. There is no gantry or other technical devices in this setup. Hence, it will not be any neutron generation before the protons hits the water phantom. This results in a reduced neutron fluence compared to the real scenario (Paganetti 2012). This experiment does therefore not tell anything about how the equipment influence the neutron production. This could influence the energy spectrum of the neutrons hitting the wall, and thereby influence the neutron penetration depth. However, neutrons generated in the equipment will also be limited in the same way as those generated in the phantom by the proton beam energy. Since the neutrons are generated by inelastic scattering from protons, the secondary particles may never have higher energy than the primary protons.

The statistics in the deeper regions of the wall is too bad. In figure 5.1 we can see that the standard deviation increases dramatically at different points in the wall for different energies, corresponding to the decrease in neutron fluence. This could have been dealt with by using biasing. By using splitting for the later regions in the wall, the number of histories would have been increased, thereby reducing the uncertainties in both the fluence graphs and the energy spectra. If there had been more time, there would have been done more attempts to implement biasing in the simulations. The duration of the simulations were already pushed to the limit, as the longest duration time was at almost twelve hours. However, only increasing the number of histories could hardly have solved the problem. To maintain a high enough number of neutrons throughout the entire wall would have demanded an increase of primary particles in several or-

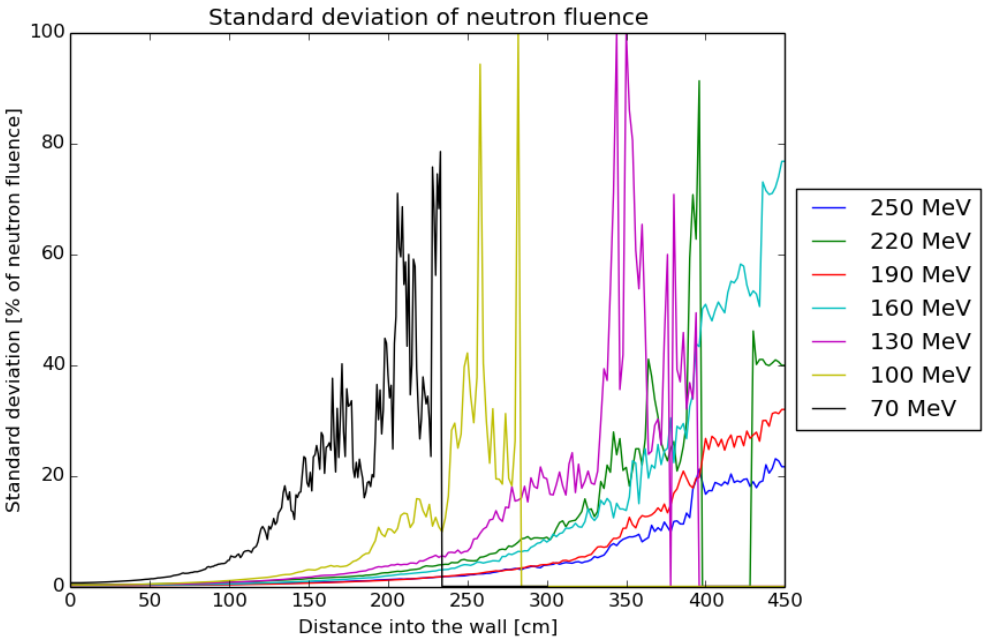

Figure 5.1: Standard deviation for the fluence as a function of distance into the wall.

ders of magnitude for the lower proton beam energies. Biasing then gives a more convinient solution, as it makes it possible to increase the statistcs in the vital regions, not the entire experiments. Due to the researcher's lack of experience in Monte Carlo simulations the importance of biasing was not entirely understood before all the simulations were done and the time left was too short to redo all the simulations.

From figure 5.2 we can see that the generation of neutrons is significantly higher for higher proton beam energies. The higher proton energy, the longer does the protons travel through the matter. This leads to more possibilities for nuclear reactions. As the energy of the generated secondary neutron is limited by the energy of the primary proton, there are both generated more neutrons, and neutrons with higher energy. This also leads to more significant attenuation of the neutrons within the water phantom for the low energy proton beams. The neutron fluence from 70 MeV protons is only 2 % of the neutron fluence from 250 MeV protons at the wall surface. This will probably vary depending of how long distance the neutrons traverse through the phantom, or the body in a real case.

An interesting phenomenon is the build-up of neutron fluence in the beginning of the wall. This is caused by the nuclear interactions from the secondary neutrons. In the early stages of the wall, there are beeing generated more neutrons by reactions like (n,2n) than there are cap-

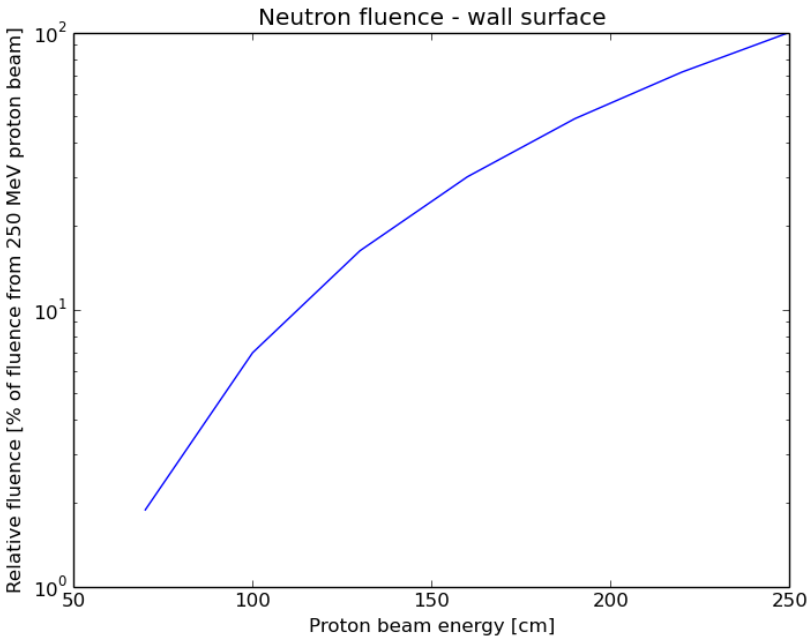

Figure 5.2: The figure shows the incoming neutron fluence hitting the inner surface of the wall.

turing of low energy neutrons. At the top of the build-up phase there are equillibrium between neutrons generated and neutrons captured. For higher proton beam energy there are generated more relativistic neutrons, that leads to more generation of neutrons. This explains the increased build-up, shown in figure 5.3, for higher energy proton beams compared to lower energy. When there are more neutrons with higher energies, there will be more neutrons capable of generating more neutrons even longer into the wall, so there will be a longer build-up phase than for lower proton beam energy. This difference in build-up distance is shown in figure 5.4.

Higher proton beam energy leads to slower neutron attenuation. The maximum energy of the neutrons are increased accordindingly to the proton beam energy. In addition, as shown in figure 5.5, the fraction of neutrons that hits the wall with high energy is increased significantly when the energy is increased and thereby amplifying the difference. This leads to that the relative difference in neutron fluence between the different proton beam energies is increasing the longer the neutrons traverse through the concrete.

When the neutrons have passed through 100 cm of concrete, the energy spectra is changed due to scattering and nuclear reactions. As seen in figure 5.6 the difference in the fraction of neutrons above 10 MeV has been more leveled for the higher energies. From figure 4.5 it is also possible to see that the high energy peak has increased compared to the thermal peak, although

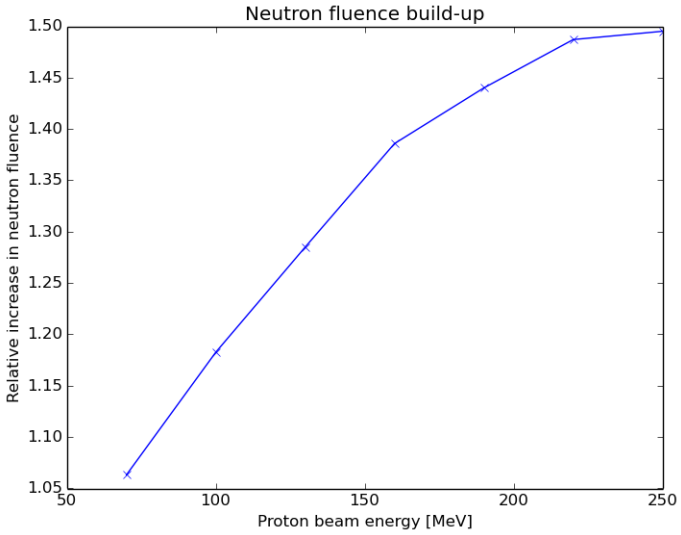

Figure 5.3: The figure shows the relative build-up in neutron fluence for different proton beam energies.

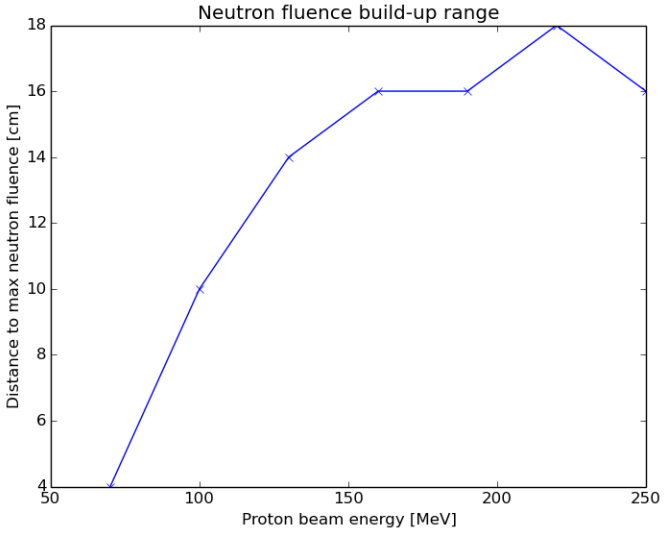

Figure 5.4: The figure shows the distance to the maximum neutron fluence for different proton beam energies.

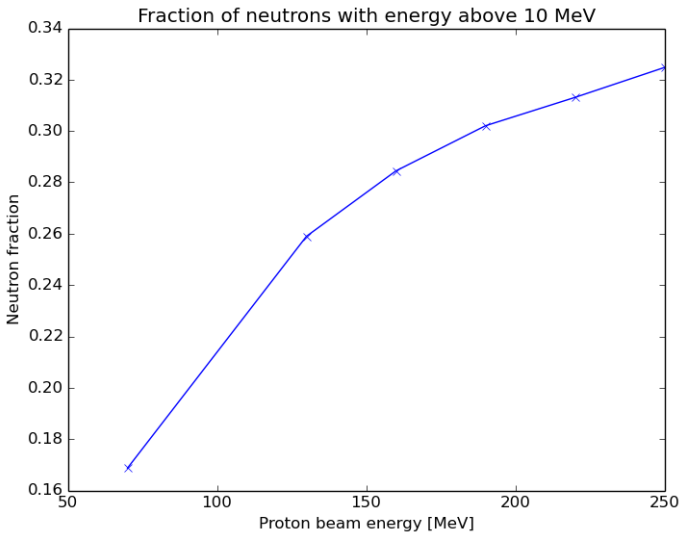

Figure 5.5: The figure shows the fraction of neutrons with energy above 10 MeV at the surface of the wall for different proton beam energies.

the thermal peak still is higher for all energies.

Figure 5.7 shows how the distance needed to reduce the neutron fluence by a certain factor varies for different energies. Due to less generation of new neutrons as the neutrons travel farther into the wall, the neutron fluence is reduced more rapidly in the deeper regions. When comparing the different energies, we can see that the distance needed to reduce the fluence is more than doubled for 250 MeV proton beam compared to 70 MeV. This comes in addition to the increased generation of neutrons for higher proton beam energies. However, the uncertainties are increasing for decreasing fluence, as shown in figure 5.8.

From this findings it is obvious that the wall dimensions needed to attenuate the neutron fluence to an acceptable level is highly dependendent of the proton beam energy that is used. Treatment rooms for ocular tumor treatment, where the proton beam energy is around 70 MeV, does not need anyway near the same shielding as a treatment room for prostate tumors at around 30 cm depth, which utilizes up to 230 MeV proton beams to attenuate the neutrons originating in the patient. The actual dimensions needed depends on a lot of factors which is not evaluated in this work.

This findings do not say anything about photon radiation due to neither neutron capture nor inelastic scattering. This will also contribute to the total radiation through the wall.

When neutrons are captured the nuclei that capture neutrons may become unstable. This

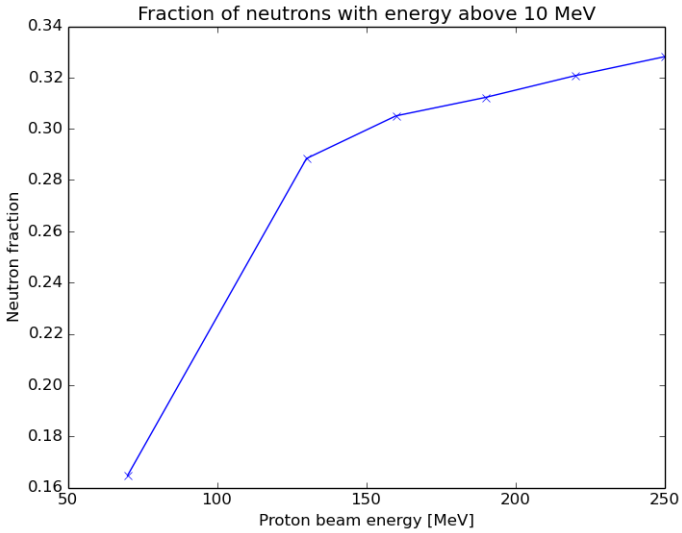

Figure 5.6: The figure shows the fraction of neutrons with energy above 10 MeV at 100 cm depth for different proton beam energies.

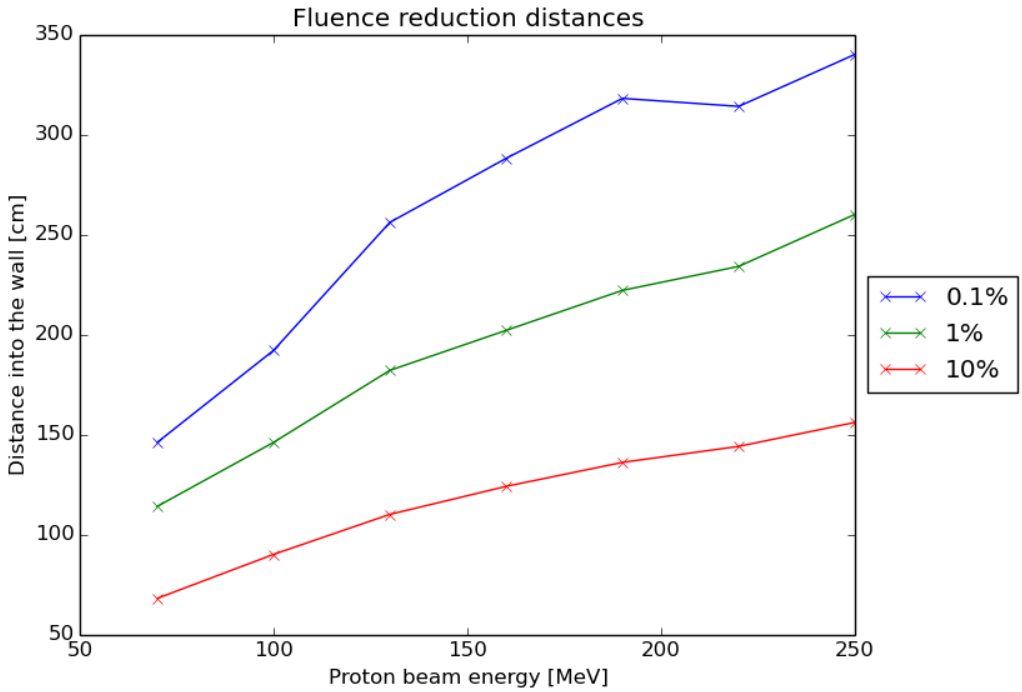

Figure 5.7: The figure shows the distance for reduction of the neutron fluence a given factor for different proton beam energies.

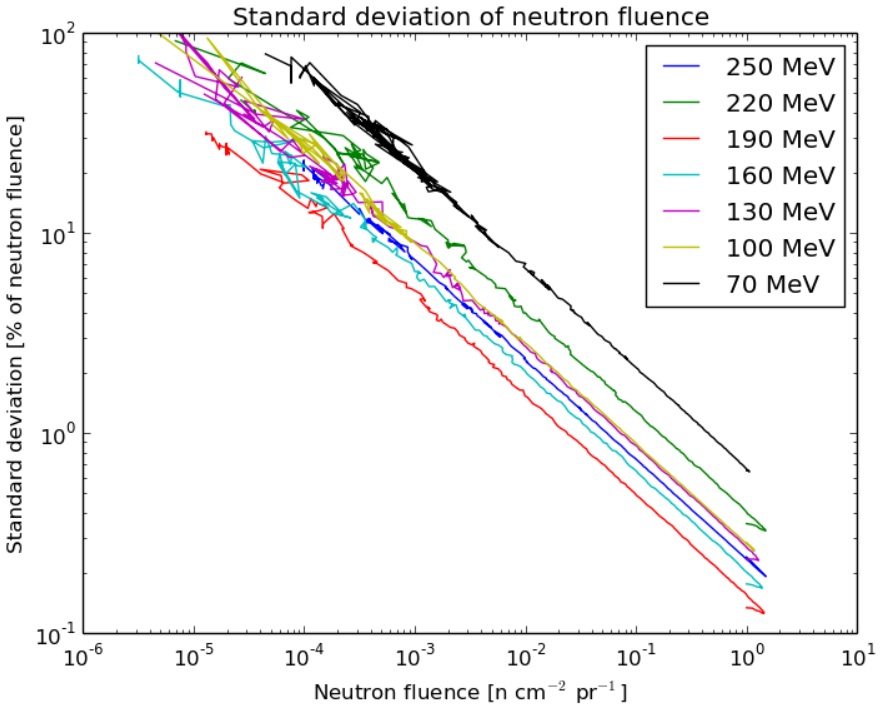

Figure 5.8: The figure shows the correlation between standard deviation in fluence and the fluence.

will lead to radiation from these unstable isotopes.

Chapter 6

Conclusion

The objective of this work was to investigate the neutron fluence through a concrete wall from neutrons originated from a proton beam irradiating a water phantom by Monte Carlo simulations.

The Monte Carlo simulations were performed with the FLUKA Monte Carlo tool. The simulations showed that the neutron attenuation is highly dependent of the proton beam energy. The neutron fluence per primary proton reaching the wall is increasing drastically with increased proton beam energy. In addition, higher proton beam energy leads to slower attenuation due to higher share of relativistic neutrons generating more neutrons and needing more collisions to be reduced to an energy level of which radiative capture is possible.

The results suffer from too bad statistics in the deeper regions of the wall. This should have been dealt with by using biasing.

Further investigation on this topic could on the short term include a similar setup with biasing. The deeper regions in the wall should be given increased importance and thereby increasing the statistics where it is needed without increasing the duration time of the simulations more than necessary.

On a longer term more aperture could be included in the geometry, taking the impact from the aperture into account. Since neutron generation from aperture has a significant impact on the total neutron generation in proton therapy, this would give valuable information that could change the amount of neutrons generated and also the energy spectrum of the neutrons.

References

Battistoni, G., Muraro, S., Sala, P. R., et al. The FLUKA code: Description and benchmarking. Hadronic shower simulation workshop 2006, 2007 Fermilab 6-8 September 2006, M. Albrow, R. Raja eds.: AIP Conference Proceeding 31-49, 2007.

Cerutti F., Battistoni G., Capezzali G., et al. Low energy nucleus-nucleus reactions: the BME approach and its interface with FLUKA Proc. 11th International Conference on Nuclear Reaction Mechanisms, Varenna (Italy) June 12-16, 2006

Gottschalk, B. 2012. Physics of Proton Interactions in Matter, Proton Therapy Physics, CRC Press - Taylor & Francis Group (21-52).

Laitano RF, Rosetti M, Frisoni M. 1996. Effects of nuclear interactions on energy and stopping power in proton beam dosimetry. Nuclear Instruments and Methods A 376:466-476

Paganetti, H. 2012. Basic Aspects of Shielding, Proton Therapy Physics, CRC Press - Taylor & Francis Group (526-536).

Suit H., Goldberg S., Niemierko A., et al. Proton Beams to Replace Photon Beams in Radical Dose Treatments, Acta Oncologica Vol. 42, No. 8, pp. 800-808, 2003

Tavernier, S. 2010, Interactions of Particles in Matter, Experimental Techniques in Nuclear and Particle Physics. (46)